J. Fluid Mech. (2009), *vol.* 630, *pp.* 179–189.
doi:10.1017/S0022112009006880 Printed in the United Kingdom

Acceleration statistics of finite-sized particles in turbulent flow: the role of Faxén forces

E. CALZAVARINI[1,4]†, R. VOLK[1,4], M. BOURGOIN[2,4], E. LÉVÊQUE[1,4], J.-F. PINTON[1,4] AND F. TOSCHI[3,4]

[1]Laboratoire de Physique de École Normale Supérieure de Lyon, CNRS et Université de Lyon, 46 Allée d'Italie, 69007 Lyon, France

[2]Laboratoire des Écoulements Géophysiques et Industriels, CNRS/UJF/INPG UMR5519, BP53, 38041 Grenoble, France

[3]Department of Physics and Department of Mathematics and Computer Science, Eindhoven University of Technology, PO Box 513, 5600 MB Eindhoven, The Netherlands

[4]International Collaboration for Turbulence Research

(Received 26 November 2008 and in revised form 9 March 2009)

The dynamics of particles in turbulence when the particle size is larger than the dissipative scale of the carrier flow are studied. Recent experiments have highlighted signatures of particles' finiteness on their statistical properties, namely a decrease of their acceleration variance, an increase of correlation times (at increasing the particles size) and an independence of the probability density function of the acceleration once normalized to their variance. These effects are not captured by point-particle models. By means of a detailed comparison between numerical simulations and experimental data, we show that a more accurate description is obtained once Faxén corrections are included.

1. Introduction

The study of Lagrangian turbulence and of turbulent transport of material particles has received growing interest in recent years (Toschi & Bodenschatz 2009). Modern experimental techniques (based on synchronization of multiple fast cameras or ultrasonic/laser Doppler velocimetry) allow nowadays to fully resolve particle tracks in turbulent flows (La Porta *et al.* 2001; Mordant *et al.* 2001; Berg 2006; Xu *et al.* 2006; Volk *et al.* 2008*b*). These techniques have opened the way towards a systematic study of the dynamics of material (or inertial) particles. When the particle density is different from the one of the carrier fluid, a rich phenomenology emerges, such as particle clustering and segregation (Squires & Eaton 1991; Calzavarini *et al.* 2008*a*,*b*). Numerical studies have proven to be essential tools in complementing and benchmarking experimental data of early days: investigations of fluid-tracer dynamics have shown remarkable agreement with experiments (Mordant, Lévêque & Pinton 2004; Arneodo *et al.* 2008; Biferale *et al.* 2008). Lagrangian numerical studies through direct numerical simulations (DNSs) of very small – computationally assumed to be pointwise – particles have also shown encouraging consistency with experimental measurements for inertial particles (Ayyalasomayajula *et al.* 2006; Bec *et al.* 2006; Salazar *et al.* 2008; Volk *et al.* 2008*a*). However, in many situations the size of the

† Email address for correspondence: enrico.calzavarini@ens-lyon.fr

particles is not small with respect to turbulence scales, in particular the dissipative scale η. One example is the plankton which, while neutrally buoyant, cannot be considered as a tracer because of its size in the order of few dissipative scales. Typical marine and atmospherical environmental flows have $\eta \sim O(10)$ μm.

The statistics of particle accelerations, which directly reflect the action of hydrodynamical forces, have been used to experimentally assess the statistical signature of 'large' spherical particles, i.e. whose diameter d is larger than the smallest turbulence scale η. Recent studies (Voth *et al.* 2002; Qureshi *et al.* 2007) and detailed comparison between experiments and numerical simulations (Volk *et al.* 2008*a*) have shown that finite-sized neutrally buoyant particles cannot be modelled as pointwise in numerical studies. Features which have been clearly associated with a finite particle size are as follows:

(i) For neutrally buoyant particles with $d > \eta$ the acceleration variance $\overline{a^2}$ decreases at increasing the particle size. A scaling law behaviour, $\overline{a^2} \sim \overline{\varepsilon}^{4/3} d^{-2/3}$ (with $\overline{\varepsilon}$ being the mean energy dissipation rate), has been suggested on the basis of Kolmogorov's (1941) turbulence phenomenology (Voth *et al.* 2002; Qureshi *et al.* 2007).

(ii) The normalized acceleration probability density function (p.d.f.) depends at best very weakly on the particle diameter. Its shape can be fitted with stretched exponential functions (see Voth *et al.* 2002; Qureshi *et al.* 2007).

(iii) The autocorrelation function of acceleration shows increased correlation time with increasing particle size (Volk *et al.* 2008*a*).

While experimentally it is easier to study large ($d > \eta$) particles, theoretically (and therefore computationally) this turns out to be a far more difficult task. Our aim in this paper is to study the novel features associated with finite particle size in developed turbulent flows while presenting an improved numerical model capable to solve most of the discrepancies between experiments and simulations noticed in Volk *et al.* (2008*a*). We show that qualitatively the new features are well captured by an equation of motion which takes into account the effect of the non-uniformity of the flow at the particle scale. To our knowledge the impact on acceleration statistics of such forces, known since a long time as Faxén corrections (Faxén 1922), has never been considered.

The paper is organized as follows: First we comment on the problems of obtaining an equation of motion for finite-sized particles. We examine the approximation on which point-particle (PP) equations rely and discuss two highly simplified models for the dynamics of small ($d < \eta$) and finite-sized ($d > \eta$) particles. Section 3 gives the numerical implementation of the proposed Faxén-corrected (FC) model. In § 4 we show basic physical differences between the statistics of particle acceleration given by numerics with or without Faxén corrections. Section 5 contains the comparison of the model against experimental results, focusing on neutrally buoyant particles. Finally in § 6 we summarize the results, critically review the model and discuss how it can be improved.

2. Equation of motion for finite-sized particle in turbulence

Many studies on fine-particulate flows have based particle's description on an equation – referred to as Maxey–Riley–Gatignol – which is an exact derivation of the forces on a particle in a non-uniform unsteady flow in the limit of vanishing Reynolds numbers $Re_p = dv_s/\nu$ and $Re_S = d^2\Gamma/\nu$, where v_s is the slip particle velocity with respect to the fluid and $\Gamma = |\nabla \boldsymbol{u}|$ the typical shear scale in the flow (Gatignol 1983; Maxey & Riley 1983). In the net hydrodynamical force acting on a particle given by

this equation one recognizes several contributions: the steady Stokes drag, the fluid acceleration force (sum of the pressure gradient and the dissipative forces on the fluid), the added mass, the buoyancy, the history Basset–Boussinesq force and Faxén corrections. When the control parameters Re_p and Re_S become finite, the nonlinearity of the flow dynamics in the vicinity of the particle must be taken into account (see the review by Michaelides 1997). An expression for the added mass term which is correct at any Re_p value has been derived by Auton, Hunt & Prud'homme (1988). But much more complicated is the situation for the other forces involved. The drag term becomes Re_p-dependent, and empirical expressions based on numerical computations have been proposed (see Clift, Grace & E. 1978). Furthermore, a lift force appears at finite values of Re_p and Re_S. This force is notably hard to model because of the nonlinear combination of shear and vorticity, and approximate expressions based on Saffman (small Re_p) and Lighthill–Auton (large Re_p) mechanisms are often used in studies (see e.g. discussion on lift on bubbles by Magnaudet & Legendre 1998).

Theoretical and numerical studies of fine disperse multi-phase flows, which aim at describing the behaviour of a large number of particles, have adopted simplified models in which the sub-dominant terms in Maxey–Riley–Gatignol equation are neglected (Balkovsky, Falkovich & Fouxon 2001; Bec 2005). A minimal model, used to address particle Lagrangian dynamics in highly turbulent suspensions, takes into account only a few ingredients: the Stokes drag, the Auton added mass and the fluid acceleration term (Babiano *et al.* 2000; Calzavarini *et al.* 2008 *b*). This leads to

$$\frac{\mathrm{d}\boldsymbol{v}}{\mathrm{d}t} = \frac{3\ \rho_f}{\rho_f + 2\ \rho_p}\left(\frac{\mathrm{D}\boldsymbol{u}}{\mathrm{D}t} + \frac{3\nu}{r^2}(\boldsymbol{u}-\boldsymbol{v})\right), \tag{2.1}$$

where ρ_f and ρ_p are respectively the fluid and the particle density, ν the fluid kinematic viscosity and $r = d/2$ the radius of the particle, which is considered spherical; $\boldsymbol{v}$ denotes the particle velocity, while $\boldsymbol{u}$ and $\mathrm{D}\boldsymbol{u}/\mathrm{D}t$ are the fluid velocity and acceleration evaluated in its centre of mass. A particle described by the above equation feels the fluid fluctuations only in one point and therefore has no real spatial extension; we may say its size r is essentially 'virtual'. Equation (2.1) indeed contains only a time scale, namely the particle relaxation time τ_p, which embodies the particle length scale merely in combination with the kinematic viscosity of the flow and with the densities coefficients, i.e. $\tau_p \equiv r^2(\rho_f + 2\ \rho_p)/(9\nu\rho_f)$. In practice, the drag term in (2.1) performs a purely temporal filtering of the flow velocity fluctuations.

It is the role of Faxén terms to account for the non-uniformity of the flow at the particle scale. Faxén forces represent necessary physical corrections when analysing the behaviour of $d > \eta$ particles in turbulence. The Faxén theorem for the drag force on a moving sphere states the relation

$$\boldsymbol{f}_D = 6\pi\nu\rho_f r\left(\frac{1}{4\pi r^2}\int_{S_p}\boldsymbol{u}(\boldsymbol{x})\ \mathrm{d}S - \boldsymbol{v}\right) = 6\pi\nu\rho_f r(\langle\boldsymbol{u}\rangle_{S_p} - \boldsymbol{v}), \tag{2.2}$$

where the integral is over surface of the sphere and $\boldsymbol{u}(\boldsymbol{x})$ the non-homogeneous steady motion of the fluid in the absence of the sphere. As later shown by Gatignol (1983), Faxén force corrections via sphere volume averages should also be included on the inertial hydrodynamic forces acting on the sphere. In particular the expression for the fluid acceleration and added mass force becomes

$$\boldsymbol{f}_A = \frac{4}{3}\pi r^3\rho_f\left(\left\langle\frac{\mathrm{D}\boldsymbol{u}}{\mathrm{D}t}\right\rangle_{V_p} + \frac{1}{2}\left(\left\langle\frac{\mathrm{d}\boldsymbol{u}}{\mathrm{d}t}\right\rangle_{V_p} - \frac{\mathrm{d}\boldsymbol{v}}{\mathrm{d}t}\right)\right), \tag{2.3}$$

where similarly as above $\langle \ldots \rangle_{V_p}$ denotes the volume average over the spherical particle. Putting together the two force contributions of (2.2) and (2.3) into an equation of motion for a sphere, $(4/3)\pi r^3 \rho_p \, \mathrm{d}\boldsymbol{v}/\mathrm{d}t = \boldsymbol{f}_D + \boldsymbol{f}_A$, and keeping into account the Auton added mass correction for finite Re_P, i.e. $\mathrm{d}\boldsymbol{u}/\mathrm{d}t \to \mathrm{D}\boldsymbol{u}/\mathrm{D}t$, we obtain the phenomenological FC equation of motion:

$$\frac{\mathrm{d}\boldsymbol{v}}{\mathrm{d}t} = \frac{3\ \rho_f}{\rho_f + 2\ \rho_p} \left(\left\langle \frac{\mathrm{D}\boldsymbol{u}}{\mathrm{d}t} \right\rangle_{V_p} + \frac{3\nu}{r^2} (\langle \boldsymbol{u} \rangle_{S_p} - \boldsymbol{v}) \right), \tag{2.4}$$

which we propose as a first-order implementation of finite-sized correction for particle dynamics. In the small particle limit, when $r \to 0$ and $\boldsymbol{u} \simeq \boldsymbol{v}$, corrections can be approximated by Taylor expansion $\langle \boldsymbol{u}(\boldsymbol{x}, t) \rangle_{S_p} \simeq \boldsymbol{u} + (r^2/6)\nabla^2 \boldsymbol{u} + O(r^4)$; $\langle \mathrm{D}\boldsymbol{u}(\boldsymbol{x}, t)/\mathrm{D}t \rangle_{V_p} \simeq (\mathrm{d}/\mathrm{d}t)(\boldsymbol{u} + (r^2/10)\nabla^2 \boldsymbol{u} + O(r^4))$; therefore the first-order Faxén correction accounts for the curvature of the unperturbed flow at the particle location. In a turbulent flow the correction term becomes important when $r > \eta$, with a weak Taylor–Reynolds number Re_λ dependence. An order of magnitude estimate is as follows: Recalling that the Taylor microscale is defined as the radius of curvature of the velocity spatial correlation function at the origin, $\lambda^2 \sim u^2/|u\nabla^2 u|$, one estimates $r^2|\nabla^2 u|/|u| \sim r^2/\lambda^2$. Now by using the relation for the dissipative scale $\eta \sim \lambda/\sqrt{Re_\lambda}$, we find $r^2|\nabla^2 u|/|u| \sim r^2/(\eta^2 Re_\lambda)$. Faxén corrections are relevant when $r \gtrsim \eta\sqrt{Re_\lambda}$, which corresponds to $r \gtrsim O(10)\ \eta$ in typical laboratory experiments ($Re_\lambda \sim O(100)$).

3. Numerical implementation of particle model and turbulence DNSs

We adopt here a further approximation which allows efficient numerical computations of (2.4). Volume averages at particles' positions are substituted by local interpolations after filtering by a Gaussian envelope with standard deviation, σ, proportional to the particle radius. Gaussian convolutions are then efficiently computed in spectral space, and the Gaussian volume averaged field reads

$$\langle u_i \rangle_{G,V_\sigma}(\boldsymbol{x}) = \mathscr{DF}\mathscr{T}^{-1}_{(N^3)}[\tilde{G}_\sigma(\boldsymbol{k})\ \tilde{u_i}(\boldsymbol{k})], \tag{3.1}$$

where $\mathscr{DF}\mathscr{T}^{-1}_{(N^3)}$ denotes a discrete inverse Fourier transform on a grid N^3; $\tilde{G}_\sigma(\boldsymbol{k}) = \exp(-\sigma^2\boldsymbol{k}^2/2)$ is the Fourier transform of a unit volume Gaussian function of variance σ; and $\tilde{u_i}(\boldsymbol{k})$ is the Fourier transform of a vector field (the material derivative of fluid velocity in (2.4)). The surface average is obtained using the exact relation

$$\langle u \rangle_{S_p} = \frac{1}{3r^2} \frac{\mathrm{d}}{\mathrm{d}r} (r^3 \langle \boldsymbol{u} \rangle_{V_p}), \tag{3.2}$$

which leads to

$$\langle u_i \rangle_{G,S_\sigma}(\boldsymbol{x}) = \mathscr{DF}\mathscr{T}^{-1}_{(N^3)}[\tilde{S}_\sigma(\boldsymbol{k})\ \tilde{u_i}(\boldsymbol{k})], \tag{3.3}$$

where $\tilde{S}_\sigma(\boldsymbol{k}) = (1-(1/3)\sigma^2\boldsymbol{k}^2)\mathrm{e}^{-(1/2)\sigma^2\boldsymbol{k}^2}$. It can be shown that with the choice $\sigma = r/\sqrt{5}$, the Gaussian convolution gives the right prefactors for the Faxén corrections in the limit $r \to 0$. Our simplified approach for the integration of (2.4) (FC model) allows to track inertial particles in turbulent flows with minimal additional computational costs as compared to (2.1) (PP model): the fluid acceleration and velocity fields are filtered once for every particle radius size; then the averaged flow at the particle positions are obtained through a trilinear interpolation. We track particles via (2.4) in a stationary homogeneous isotropic flow, generated by large-scale volume forcing

on a cubic domain. The Navier–Stokes (NS) equation is discretized on a regular grid, integrated using a pseudo-spectral algorithm and advanced in time with a second-order Adams–Bashford integrator. The spatial and temporal accuracy of the integration and its validation have been carefully examined. To ensure a good spatial resolution of NS equation we set $\eta\ k_{max} \simeq 1.7$, where k_{max} is the largest represented wave vector. For the time accuracy, controlled by the marching step δt, the Courant number is chosen to be small, $Co \equiv \boldsymbol{u}_{rms}\ k_{max}\ \delta t \simeq 0.16$. With this choice $\tau_\eta \simeq O(10^2)\ \delta t$; therefore the Lagrangian equations for particles considered in this study (all with response time $\tau_p \gtrsim \tau_\eta$) can be safely integrated with the same time stepping of the Eulerian field. We have checked the integration in simple flows cases, e.g. a two-dimensional stationary cellular flow in which the filtered particle dynamics can be derived analytically. The turbulent case instead has been validated by a comparison with an independently developed code, implementing the same equations for particles but with different forcing scheme, temporal integration method (Verlet algorithm) and local interpolation procedure (tricubic algorithm).

We have explored in a systematic way the two-dimensional parameter space $[\rho_p/\rho_f, d/\eta]$ in the range $\rho_p/\rho_f \in [0.1, 10]$ and $d/\eta \in [2, 50]$ for a turbulent flow at $Re_\lambda = 180$ (512^3 collocation points). We tracked $\sim 2 \times 10^6$ particles for a total of ~ 4 large-eddy turnover times in statistically stationary conditions. Lower-resolution DNSs at $Re_\lambda = 75$ (128^3) have been used to explore a larger parameter space and to study the differences between the PP model (2.1) and the FC model (2.4) in the asymptote $d \to L$ (with L the turbulence integral scale).

4. Phenomenology of PP and FC models

We compare the statistics of acceleration of particles tracked via the PP and FC equations. In the small particle limit ($d/\eta \to 0$) the two model equations behave the same way, and the particle trajectory becomes the one of a fluid tracer. The ensemble-average acceleration variance reaches the value $\overline{a^2} \to \overline{a_f^2}$ with the subscript f labelling the fluid tracer acceleration. As the particle diameter is increased we notice important differences between the two models. In the PP model the drag term becomes negligible, and one gets $\overline{a^2} \simeq \beta^2 \overline{a_f^2}$, with $\beta = 3\rho_f/(\rho_f + 2\rho_p)$. In the FC model the volume average of the fluid acceleration $\mathrm{D}\boldsymbol{u}/\mathrm{D}t$ reduces progressively the particle acceleration. This is illustrated in figure 1(*a*), where the particle acceleration variance (normalized by $\beta^2\overline{a_f^2}$) is shown for three cases: neutral buoyant, heavy ($\rho_p/\rho_f = 10$) and light ($\rho_p/\rho_f = 0.1$) particles. (The effect of gravity is here assumed negligible compared to the one of turbulent fluctuations.) We note that the behaviour of $\overline{a^2}$ for particles whose diameter is roughly larger than 10η seems to be identical apart from the scaling factor β^2.

Differences are also present in higher-order moments: for this we focus on the flatness $F(a) \equiv \overline{a^4}/(\overline{a^2})^2$. In the large d limit PP model gives the rather unphysical behaviour $F(a) \simeq F(a_f)$; that is to say large particles, irrespectively of their density, show the same level of intermittency as a fluid tracer. On the other hand the FC equation gives asymptotically $F(a) \simeq 3$, i.e. the Gaussian flatness value, meaning that acceleration of large particles independent of their mass density value has lost its intermittent character (see figure 1*b*). Furthermore, it is noticeable that above a certain critical value of the diameter the flatness of heavy/neutral and light particles

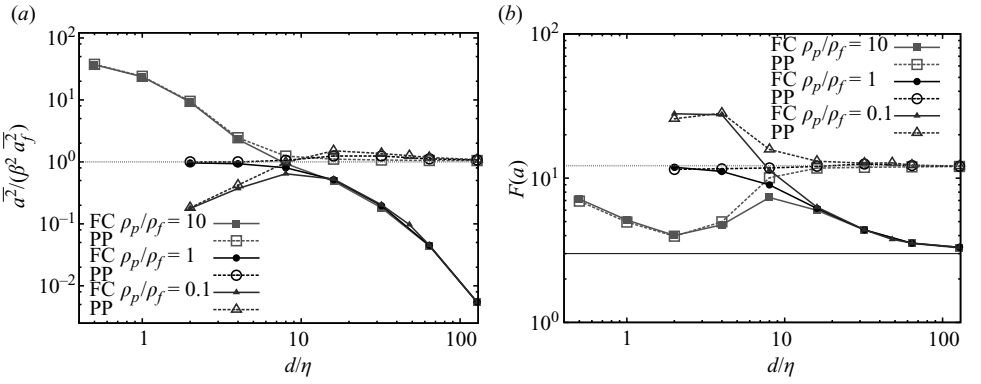

FIGURE 1. (*a*) The acceleration variance $\overline{a^2}$ normalized by $\beta^2\overline{a_f^2}$ versus the particle diameter as derived from the FC model (solid lines/symbols) and from PP the model system (dashed lines/empty symbols). Density ratios shown are $\rho_p/\rho_f = 0.1, 1, 10$, i.e. heavy (□), neutral (○) and light (△) particles. (*b*) Same as above for the acceleration flatness $F(a) = \overline{a^4}/(\overline{a^2})^2$. Horizontal lines shows the flatness of the fluid acceleration $F(a_f)$ and the flatness value for Gaussian distribution $F(a) = 3$. Data from simulations at $Re_\lambda = 75$.

reaches the same level: this suggests that also the p.d.f.s may have very similar shapes.

5. Comparison with experiments for neutrally buoyant particles

We study now how the FC model compares with the experimental observations listed in the introduction – recalling than none is captured by the PP model.

5.1. *Acceleration variance*

In figure 2 the behaviour of the one-component acceleration variance, normalized by the Heisenberg–Yaglom scaling, $a_0 = \overline{a_i^2}\,\overline{\varepsilon}^{-3/2}\nu^{1/2}$, is displayed. Although this way of normalizing the acceleration has a weak Reynolds number dependence (see Voth *et al.* 2002; Bec *et al.* 2006) we notice a very similar behaviour as compared to the experimental measurements at $Re_\lambda = 160$ by Qureshi *et al.* (2007) and the $Re_\lambda = 970$ experiments by Voth *et al.* (2002). In the inset of figure 2 the same quantity but with a different normalization is shown. The particle acceleration variance there is divided by the second moment of fluid tracer acceleration $\overline{a_f^2}$. The experimental data from Voth *et al.* (2002) can also be rescaled in the same way by dividing a_0 by the value for the smallest considered particle (which has size $d \simeq 1.44\eta$ and essentially behaves as a fluid tracer). This alternate way of looking at the data renormalizes the weak Re_λ dependence, providing a good agreement between the DNSs and experiments even when comparing results with one order of magnitude difference in Re_λ.

In a DNS one can estimate the relative weight of the terms contributing to the total acceleration: the drag and fluid acceleration terms, respectively, $a^D = (\langle \boldsymbol{u}\rangle_{S_p} - \boldsymbol{v})/\tau_p$ and $a^A = \beta\langle \mathrm{D}\boldsymbol{u}/\mathrm{D}t\rangle_{V_p}$. It is important to note that in the case of neutrally buoyant particles, one finds $\overline{a^2} \simeq \overline{(a^A)^2}$ with per cent accuracy. It indicates that the observed effect – decrease of particle acceleration variance for increasing particle diameter – comes uniquely from volume averaging of fluid acceleration at the particle position. The drag contribution is sub-leading at all d values (from few per cent up to 15 % of total acceleration variance); it just contributes to compensate the $a^D a^A$ correlations.

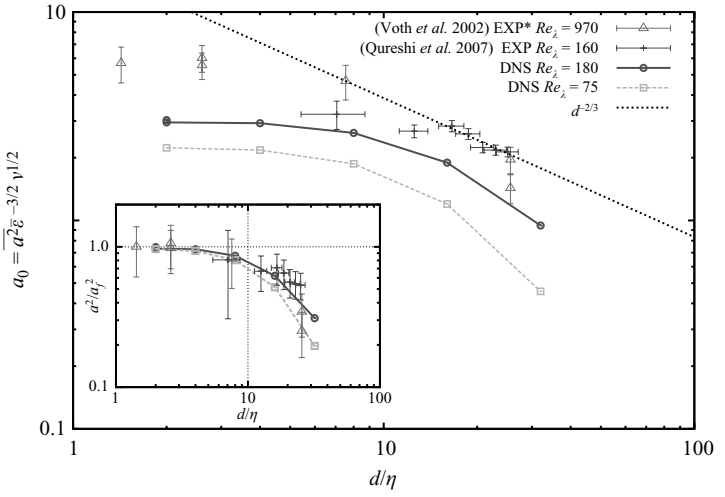

FIGURE 2. One-component acceleration variance versus particle size. Acceleration is normalized by the Heisenberg–Yaglom relation, while the particle size is normalized by the dissipative scale. DNS results have uncertainty of the order of the symbol size. Experimental data (EXP) are from Qureshi *et al.* (2007), with experimental measurement (EXP*) from (Voth *et al.* 2002, figure 32)–particles with density contrast $\rho_p/\rho_f = 1.06$. Inset: $\overline{a^2}/\overline{a_f^2}$ versus d/η from the same DNS and experimental (EXP*) measurements.

Stated differently, one can say that the acceleration of a finite-sized neutrally buoyant particle is essentially given by $\langle \mathrm{D}\boldsymbol{u}/\mathrm{D}t \rangle_{V_p} = \langle \boldsymbol{\nabla} \cdot \boldsymbol{\tau} + \boldsymbol{f}_e \rangle_{V_p} \simeq (1/3r) \langle \boldsymbol{\tau} \cdot \boldsymbol{n} \rangle_{S_p}$, where $\boldsymbol{\tau}$ is the stress tensor, $\boldsymbol{n}$ a unit norm vector pointing outward the sphere and $\boldsymbol{f}_e$ the external large-scale forcing whose contribution $\langle \boldsymbol{f}_e \rangle_{V_p} \simeq 0$ is negligible at the particle scale. One expects the situation to be different for particles whose densities do not match that of the fluid.

Our simulations are consistent with the $a_0 \sim d^{-2/3}$ scaling which has been proposed on the basis of dimensional arguments rooted on K41 turbulence phenomenology without special assumptions of particle dynamics (Voth *et al.* 2002; Qureshi *et al.* 2007); however at $Re_\lambda = 180$ the scale separation is still too limited to observe a true scaling range.

5.2. *Acceleration p.d.f.*

The second quantity under study is the acceleration p.d.f. Here, to cope with Re_λ effects, one compares only the two most similar data sets: the DNS at $Re_\lambda = 180$ and the experiment at $Re_\lambda = 160$ (Qureshi *et al.* 2007). Experiments have revealed a universal behaviour for acceleration p.d.f. normalized by $(\overline{a_i^2})^{1/2}$ in the size range $d = 12$–25η. DNS instead shows a systematic difference in its trend: larger particles have less intermittent acceleration statistics (see figure 3*a*). However, the shape of the p.d.f. in the limit of large particles $d \simeq 30\eta$ shows a good similarity. To better visualize differences, in figure 3(*b*), we show the flatness $F(a)$ versus particle diameter for DNSs and experiments. As already observed, the FC model leads to decreasing intermittency for bigger neutral particles and in the asymptotic limit ($d \to L$) to Gaussian distribution; also acceleration flatness is an increasing function of Re_λ. The experiment of Qureshi and co-workers' (2007) on the other hand showed a d-independent behaviour around $F(a) = 8.5$. A further possible source of differences can be connected to the variations in the large-scale properties of turbulent flows:

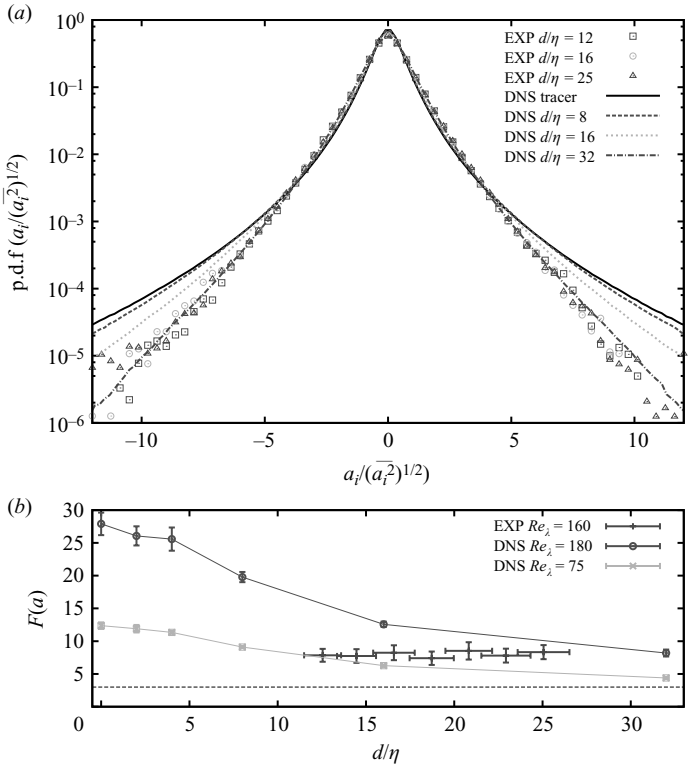

FIGURE 3. (*a*) Comparison of p.d.f.s of acceleration normalized by its r.m.s. value, from Qureshi *et al.* (2007), denoted by EXP, at $Re_\lambda = 160$ and DNS at $Re_\lambda = 180$. (*b*) One-component acceleration flatness $F(a) = \overline{a_i^4}/(\overline{a_i^2})^2$ versus the normalized particle diameter d/η from the same experiment and DNS at two different Reynolds numbers.

experimental tracks come from a decaying grid-generated turbulence; simulations instead uses volume large-scale forced flow in a cubic domain without mean flow.

5.3. *Acceleration time correlation*

Finally, we consider the dynamics of the neutral particles. We study the normalized one-component correlation function, $C_{aa}(\tau) \equiv \overline{a_i(t)a_i(t+\tau)}/\overline{a_i^2}$. In Volk *et al.* (2008*a*) it has been noted that PP model cannot account for the increasing autocorrelation for larger particles. This is understood from (2.1): In the large d/η limit the drag term is negligible, and the acceleration of a neutrally buoyant particle is dominated by the inertial term $\mathrm{D}\boldsymbol{u}/\mathrm{D}t$. Therefore the time correlation of acceleration, $C_{aa}(\tau)$, is related to the temporal correlation of $\mathrm{D}\boldsymbol{u}/\mathrm{D}t$ along the particle trajectory. Because in the large d limit $\boldsymbol{v} \neq \boldsymbol{u}$ (Babiano *et al.* 2000), one expects an acceleration correlation time which is equal to or even shorter than the one of a fluid tracer. This is confirmed by our numerics based on the PP equation (2.1). In the FC model instead, the averaged quantity $\langle \mathrm{D}\boldsymbol{u}/\mathrm{D}t \rangle_{V_p}$ dominates the particle's acceleration and also its time correlation $C_{aa}(\tau)$. In figure 4 we show that simulations based on (2.4) display increasing correlation time for bigger particles, as observed in experiment (Volk *et al.* (2008*a*) although at much larger Re_λ values. A detailed comparison of the $C_{aa}(\tau)$ curves coming from DNSs with experiments by Qureshi and co-workers (2007) is at present not possible, because of limited statistics. Therefore, we examine integral

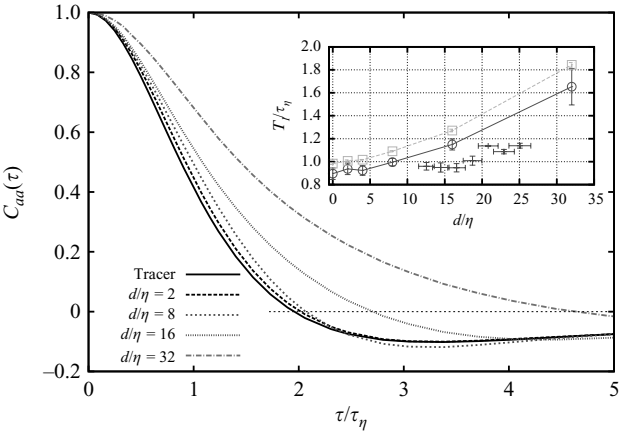

FIGURE 4. Autocorrelation function of acceleration $C_{aa}(\tau)$ for neutral particles ($\rho_p = \rho_f$), with different sizes $d = 2\eta, 8\eta, 16\eta, 32\eta$ and a tracer particle; zoom for $\tau/\tau_\eta < 5$; asymptotically all the curves go to zero. Inset: integral acceleration time $T_I = \int_0^{T_0} C_{aa}(\tau)\, \mathrm{d}\tau$, with T_0 the zero-crossing time, $C_{aa}(T_0) = 0$, versus particle diameter. Symbols: (□, ○) DNS at $Re_\lambda = (75, 180)$; (+) data from experiments at $Re_\lambda = 160$.

quantities such as an integral acceleration time T_I. Since by kinematic constraint the time integral of $C_{aa}(\tau)$ for a small tracer is zero, we define T_I as the integral over time of the positive part of $C_{aa}(\tau)$; this choice proves to be stable in the experiments and weakly dependent on the unavoidable (Gaussian) smoothing of noisy data sets (see Volk *et al.* 2008*b*). The result of this analysis is reported in figure 4 (inset). The order of magnitude of T_I/τ_η, which is very near unity, as well its increasing trend with d qualitatively confirm the prediction of the FC model at similar Reynolds number. Using DNS results, it is also interesting to note that this time decreases with increasing Reynolds number.

6. Discussion of results and conclusions

We have investigated the origin of several experimental observations concerning neutrally buoyant finite-sized particle acceleration in turbulent flows and shown the relevance of Faxén corrections. Faxén terms account for inhomogeneities in the fluid flow at the spatial extension of the particle. They act as spatial coarse graining of the surrounding turbulent flow, in contrast with the drag term which performs a temporal filtering. Numerically, the spatial average is efficiently implemented via Gaussian filtering in spectral space. Comparing with experimental measurements, the main achievements of the FC model are (i) prediction of the reduction of acceleration fluctuations at increasing the particle size and (ii) prediction of the increasing of acceleration time correlation at increasing the particle size. Both effects originate from the volume average of the fluid acceleration term or in other word from the surface average of the stress tensor of the unperturbed flow. While the FC model gives the correct trend, it does not solve the puzzling point of invariant p.d.f. with particle size, observed by Qureshi *et al.* (2007).

The FC model improves the statistical description of realistic turbulent particle suspensions. We emphasize that none of the observed trends in the acceleration of neutrally buoyant particles can be captured by previous purely local models, as e.g. the PP one in (2.1). Faxén corrections are of special relevance in the case of neutrally

buoyant particles, because it is the case for which the slip velocity ($v_s \equiv |\boldsymbol{v} - \langle \boldsymbol{u} \rangle_{S_p}|$) is the smallest (as compared to $\rho_p \neq \rho_f$ particles) and therefore in which drag, history and lift have the least impact on the net force. In our case we observe that when increasing the size of particles, the p.d.f.s of slip velocity normalized by the fluid velocity root mean square (r.m.s.) value ($v_s/\boldsymbol{u}_{rms}$) change from a sharp delta-like shape (for tracers) to larger distributions approaching a Gaussian (for large particles). A size-dependent slip velocity for neutrally buoyant particles in chaotic flows has been reported recently in Ouellette, O'Malley & Gollub (2008): Faxén corrections to the added mass should be significant in that case too. We also observe that the particle Reynolds number Re_p measured in our simulations reaches values $O(100)$; hence a more accurate description of the drag force on a sphere in a turbulent environment (see for instance Bagchi & Balachandar 2003) may be important particularly for a faithful reproduction of the far tails of the acceleration p.d.f.

The authors acknowledge the Grenoble team (N. M. Qureshi, C. Baudet, A. Cartellier and Y. Gagne) for generously sharing their experimental data measurements and J. Bec for useful discussions. Numerics have been performed at SARA (The Netherlands), CINECA (Italy) and PSMN at ENS-Lyon (France). Numerical raw data on FC particles are freely available on the iCFDdatabase (http://cfd.cineca.it) kindly hosted by CINECA (Italy).

REFERENCES

Arneodo, A., Benzi, R., Berg, J., Biferale, L., Bodenschatz, E., Busse, A., Calzavarini, E., Castaing, B., Cencini, M., Chevillard, L., Fisher, R., Grauer, R., Homann, H., Lamb, D., Lanotte, A. S., Leveque, E., Luthi, B., Mann, J., Mordant, N., Muller, W.-C., Ott, S., Ouellette, N. T., Pinton, J.-F., Pope, S. B., Roux, S. G., Toschi, F., Xu, H. & Yeung, P. K., ICTR Collaboration 2008 Universal intermittent properties of particle trajectories in highly turbulent flows. *Phys. Rev. Lett.* **100** (25), 254504–254505.

Auton, T., Hunt, J. & Prud'homme, M. 1988 The force exerted on a body in inviscid unsteady non-uniform rotational flow. *J. Fluid Mech.* **197**, 241–257.

Ayyalasomayajula, S., Gylfason, A., Collins, L. R., Bodenschatz, E. & Warhaft, Z. 2006 Lagrangian measurements of inertial particle accelerations in grid generated wind tunnel turbulence. *Phys. Rev. Lett.* **97**, 144507.

Babiano, A., Cartwright, J. H. E., Piro, O. & Provenzale, A. 2000 Dynamics of a small neutrally buoyant sphere in a fluid and targeting in Hamiltonian systems. *Phys. Rev. Lett.* **84** (25), 5764–5767.

Bagchi, P. & Balachandar, S. 2003 Effect of turbulence on the drag and lift of a particle. *Phys. Fluids.* **15** (11), 3496–3513.

Balkovsky, E., Falkovich, G. & Fouxon, A. 2001 Intermittent distribution of inertial particles in turbulent flows. *Phys. Rev. Lett.* **86** (13), 2790–2793.

Bec, J. 2005 Multifractal concentrations of inertial particles in smooth random flows. *J. Fluid Mech.* **528**, 255–277.

Bec, J., Biferale, L., Boffetta, G., Celani, A., Cencini, M., Lanotte, A., Musacchio, S. & Toschi, F. 2006 Acceleration statistics of heavy particles in turbulence. *J. Fluid Mech.* **550**, 349–358.

Berg, J. 2006 Lagrangian one-particle velocity statistics in a turbulent flow. *Phys. Rev.* E **74**, 016304.

Biferale, L., Bodenschatz, E., Cencini, M., Lanotte, A. S., Ouellette, N. T., Toschi, F. & Xu, H. 2008 Lagrangian structure functions in turbulence: a quantitative comparison between experiment and direct numerical simulation. *Phys. Fluids* **20** (6), 065103.

Calzavarini, E., Cencini, M., Lohse, D. & Toschi, F. 2008*a* Quantifying turbulence-induced segregation of inertial particles. *Phys. Rev. Lett.* **101**, 084504.

Calzavarini, E., Kerscher, M., Lohse, D. & Toschi, F. 2008*b* Dimensionality and morphology of particle and bubble clusters in turbulent flow. *J. Fluid Mech.* **607**, 13–24.

Clift, R., Grace, J. R. & Weber, M. E. 1978 *Bubbles, Drops and Particles*. Academic.

Faxén, H. 1922 Der Widerstand gegen die Bewegung einer starren Kugel in einer zähen Flüssigkeit, die zwischen zwei parallelen ebenen Wänden eingeschlossen ist, *Annalen der Physik* **373** (10), 89–119.

Gatignol, R. 1983 The Faxén formulae for a rigid particle in an unsteady non-uniform stokes flow. *J. Mec. Theor. Appl.* **1** (2), 143–160.

Kolmogorov, A. N. 1941 The local structure of turbulence in incompressible viscous fluid for very large Reynolds numbers. *Proc. USSR Acad. Sci.* **30**, 299–303.

La Porta, A., Voth, G. A., Crawford, A. M., Alexander, J. & Bodenschatz, E. 2001 Fluid particle accelerations in fully developed turbulence. *Nature* **409**, 1017.

Magnaudet, J. & Legendre, D. 1998 Some aspects of the lift force on a spherical bubble. *Appl. Sci. Res.* **58**, 441.

Maxey, M. R. & Riley, J. J. 1983 Equation of motion for a small rigid sphere in a non-uniform flow. *Phys. Fluids* **26** (4), 883–889.

Michaelides, E. E. 1997 Review – the transient equation of motion for particles, bubbles, and droplets. *J. Fluid Eng.* **119**, 233–247.

Mordant, N., Lévêque, E. & Pinton, J. F. 2004 Experimental and numerical study of the Lagrangian dynamics of high Reynolds turbulence. *New J. Phys.* **6**, 116.

Mordant, N., Metz, P., Michel, O. & Pinton, J.-F. 2001 Measurement of Lagrangian velocity in fully developed turbulence. *Phys. Rev. Lett.* **87** (21), 214501.

Ouellette, N. T., O'Malley, P. J. J. & Gollub, J. P. 2008 Transport of finite-sized particles in chaotic flow. *Phys. Rev. Lett.* **101**, 174504.

Qureshi, N. M., Bourgoin, M., Baudet, C., Cartellier, A. & Gagne, Y. 2007 Turbulent transport of material particles: an experimental study of finite size effects. *Phys. Rev. Lett.* **99** (18), 184502.

Salazar, J., de Jong, J., Cao, L., Woodward, S., Meng, H. & Collins, L. 2008 Experimental and numerical investigation of inertial particle clustering in isotropic turbulence. *J. Fluid Mech.* **600**, 245–256.

Squires, K. D. & Eaton, J. K. 1991 Preferential concentration of particles by turbulence. *Phys. Fluids* A **3** (5), 1169–1179.

Toschi, F. & Bodenschatz, E. 2009 Lagrangian properties of particles in turbulence. *Annu. Rev. Fluid Mech.* **41**, 375–404.

Volk, R., Calzavarini, E., Verhille, G., Lohse, D., Mordant, N., Pinton, J. F. & Toschi, F. 2008*a* Acceleration of heavy and light particles in turbulence: comparison between experiments and direct numerical simulations. *Physica* D **237** (14–17), 2084–2089.

Volk, R., Mordant, N., Verhille, G. & Pinton, J. F. 2008*b* Laser doppler measurement of inertial particle and bubble accelerations in turbulence. *Europhys. Lett.* **81** (3), 34002.

Voth, G. A., La Porta, A., Crawford, A. M., Alexander, J. & Bodenschatz, E. 2002 Measurement of particle accelerations in fully developed turbulence. *J. Fluid Mech.* **469**, 121–160.

Xu, H., Bourgoin, M., Ouellette, N. T. & Bodenschatz, E. 2006 High order Lagrangian velocity statistics in turbulence. *Phys. Rev. Lett.* **96** (2), 024503.